FIGURE S1

dsb-2

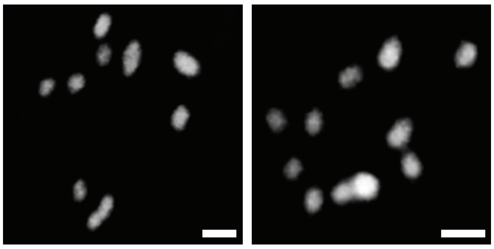

Figure S1 The *dsb-2* mutant shows a shortage in chiasmata. The lack of chiasmata revealed by univalents in diakinesis nuclei, as previously reported (ROSU et al. 2013). Representative DAPI-stained diakinesis nuclei of *dsb-2* mutants at day 2 of adulthood. Scale bars= 2μm.

FIGURE S2

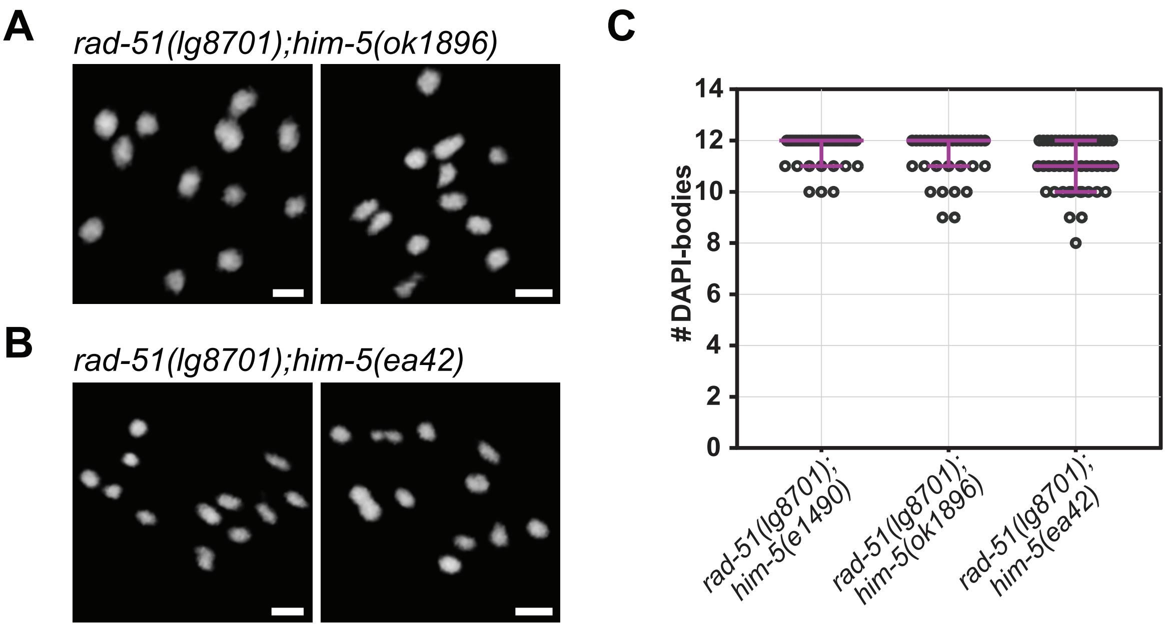

Figure S2 Suppression of *rad-51* chromosomes fusions by *him-5* is not allele-specific. (A-C) Multiple alleles of *him-5* suppress the formation of chromosomal fusions that normally arise when *rad-51* is mutated. (A, B) Represenative images and (C) Quantificationof DAPI-stained diakinesis nuclei in two-day-old adults of indicated genotypes. Scale bars= 2μm. Magenta bars indicate the median and the interquartile range. P-values from Kruskal-Wallis multiple comparison are indicated on top of the graph (n.s.: not significant, P>0.11). *rad-51(lg8701);him-5(e1490)* (n=33), *rad-51(lg8701);him-5(ok1896)* (n=32) and *rad-51(lg8701);him-5(ea42)* (n=47).

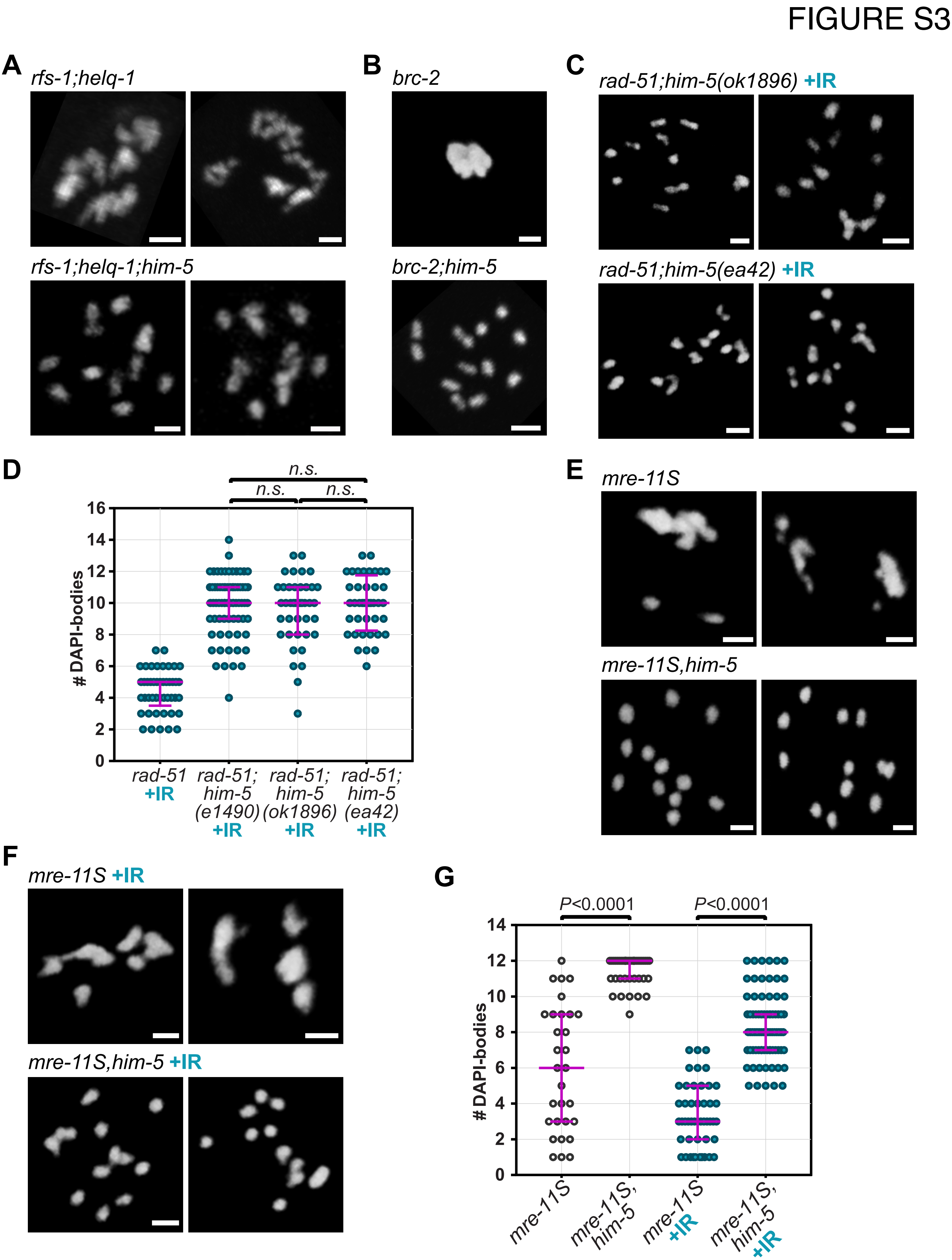

FIGURE S3
A
rfs-1;helq-1
rfs-1;helq-1;him-5
B
brc-2
brc-2;him-5
C
rad-51;him-5(ok1896) +IR
rad-51;him-5(ea42) +IR
D
n.s.
n.s.
n.s.
DAPI-bodies
16
14
12
10
8
6
4
2
0
rad-51 +IR
rad-51; him-5 (e1490) +IR
rad-51; him-5 (ok1896) +IR
rad-51; him-5 (ea42) +IR
E
mre-11S
mre-11S,him-5
F
mre-11S +IR
mre-11S,him-5 +IR
G
P<0.0001
P<0.0001
DAPI-bodies
14
12
10
8
6
4
2
0
mre-11S
mre-11S, him-5
mre-11S +IR
mre-11S, him-5 +IR

Figure S3 The depletion of *him-5* suppresses chromosomes fusions caused by mutations in genes encoding proteins required for strand-exchange. (A) *rfs-1;helq-1* and (B) *brc-2* mutant animals exhibit chromosomal clumping at diakinesis that is suppressed by the depletion of *him-5*. (C, D) Irradiation of *rad-51;him-5* does not restore a *rad-51*-like phenotype (C) Representative images and (D) Quantification of diakinesis nuclei from two-day-old irradiated animals: *rad-51(lg8701)* (n=45), *rad-51(lg8701);him-5(e1490)* (n=71), *rad-51(lg8701);him-5(ok1896)* (n=40), and *rad-51(lg8701);him-5(ea42)* (n=40). Kruskal-Wallis multiple comparison indicate that irradiated double mutants are indistinguishable from each other (*n.s.*: not significant, *P*>0.9999). (E-G) Diakinesis nuclei of *mre-11S,him-5* double mutants contain univalents than are not suppressed by IR-induced breaks. (E-F) Diakinesis nuclei of two-day-old adults without and with (+) IR. Scale bars= 2µm. (G) Quantification of DAPI bodies in diakinesis nuclei of different genotypes: unirradiated (clear dots) *mre-11S(iow1)* (n=30), *mre-11S(iow1);him-5(e1490)* (n=39), and irradiated (+IR, blue dots) *mre-11S(iow1)* (n=47) and *mre-11S(iow1);him-5(e1490)* (n=79). *P*-values calculated by two-tailed Mann-Whitney tests. Magenta bars indicate median and interquartile range (D, G).

FIGURE S4

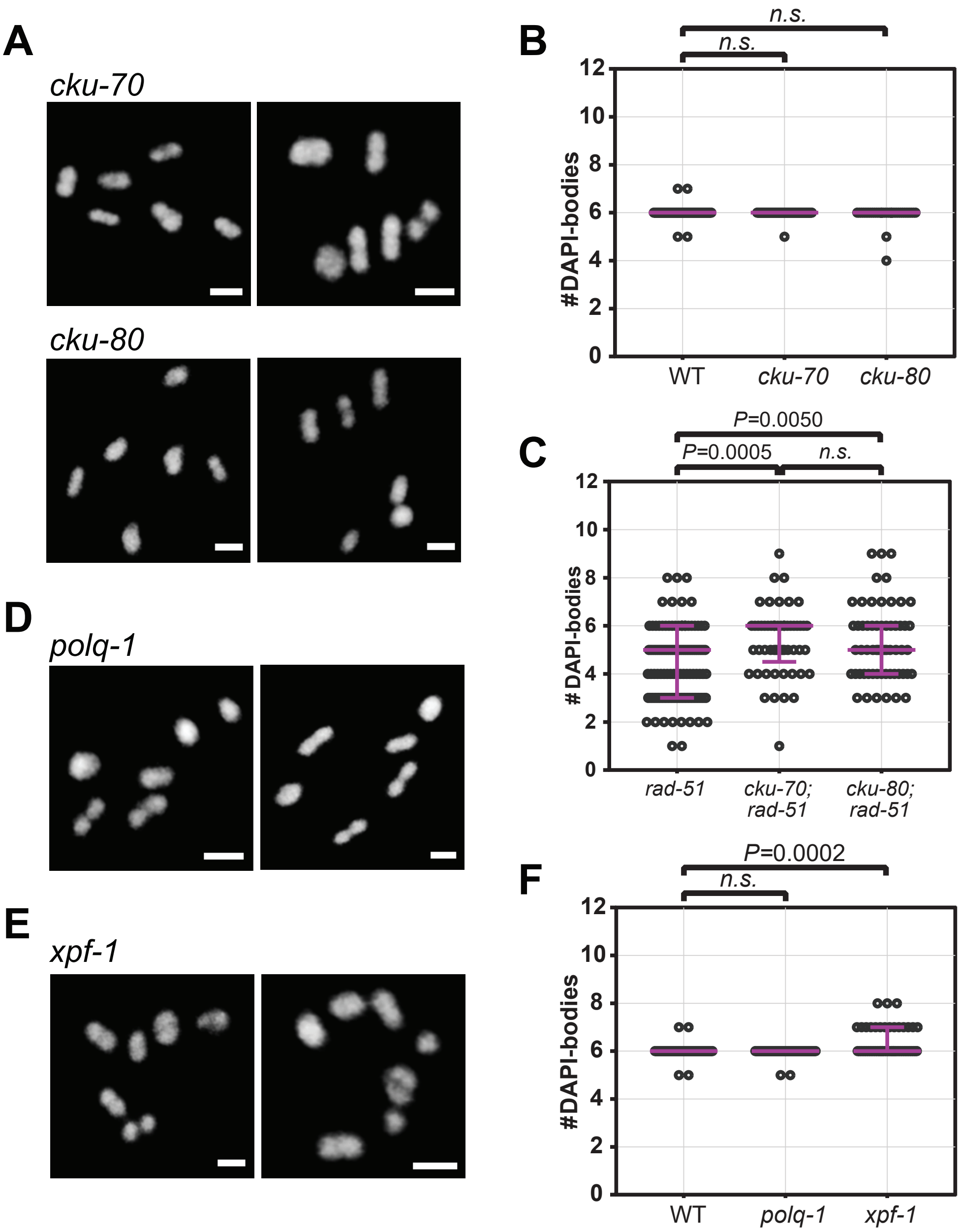

Figure S4 Mild to no crossover defects are observed in animals carrying single mutations in non-HR repair genes. (A, B) Diakinesis nuclei of mutants for Ku-complex components contain six ovoid DAPI-stained bodies and are indistinguishable from nuclei of wild-type worms. (A) Representative images and (B) Quantification of diakinesis oocytes in one-day-old adults. (C) Impairment of c-NHEJ partially suppresses the formation of chromatin fusions in *rad-51* mutant animals, increasing the number of DAPI-dense structures in diakinesis nuclei. (D) Depletion of *polq-1* does not affect crossover formation by itself as six bivalents are seen in all nuclei. (E) Univalents are seen occasionally in xpf-1 mutant animals. DAPI-stained diakinesis nuclei at day 2 of adulthood. Scale bars= 2*μ*m. (F) Quantification of DAPI-bodies in diakinesis nuclei. Magenta bars indicate the median and the interquartile range. Two-tailed Mann-Whitney tests (n.s.: not significant, P>0.19). Wild type (WT, n=45), cku-70(tm1524) (n=40), cku-80(ok851) (n=32), polq-1(tm2026) (n=45), xpf-1(e1487) (n=55), rad-51(lg8701) (n=106), cku-70(tm1524);rad-51(lg8701) (n=53), cku-80(ok851);rad-51(lg8701) (n=58).

FIGURE S5

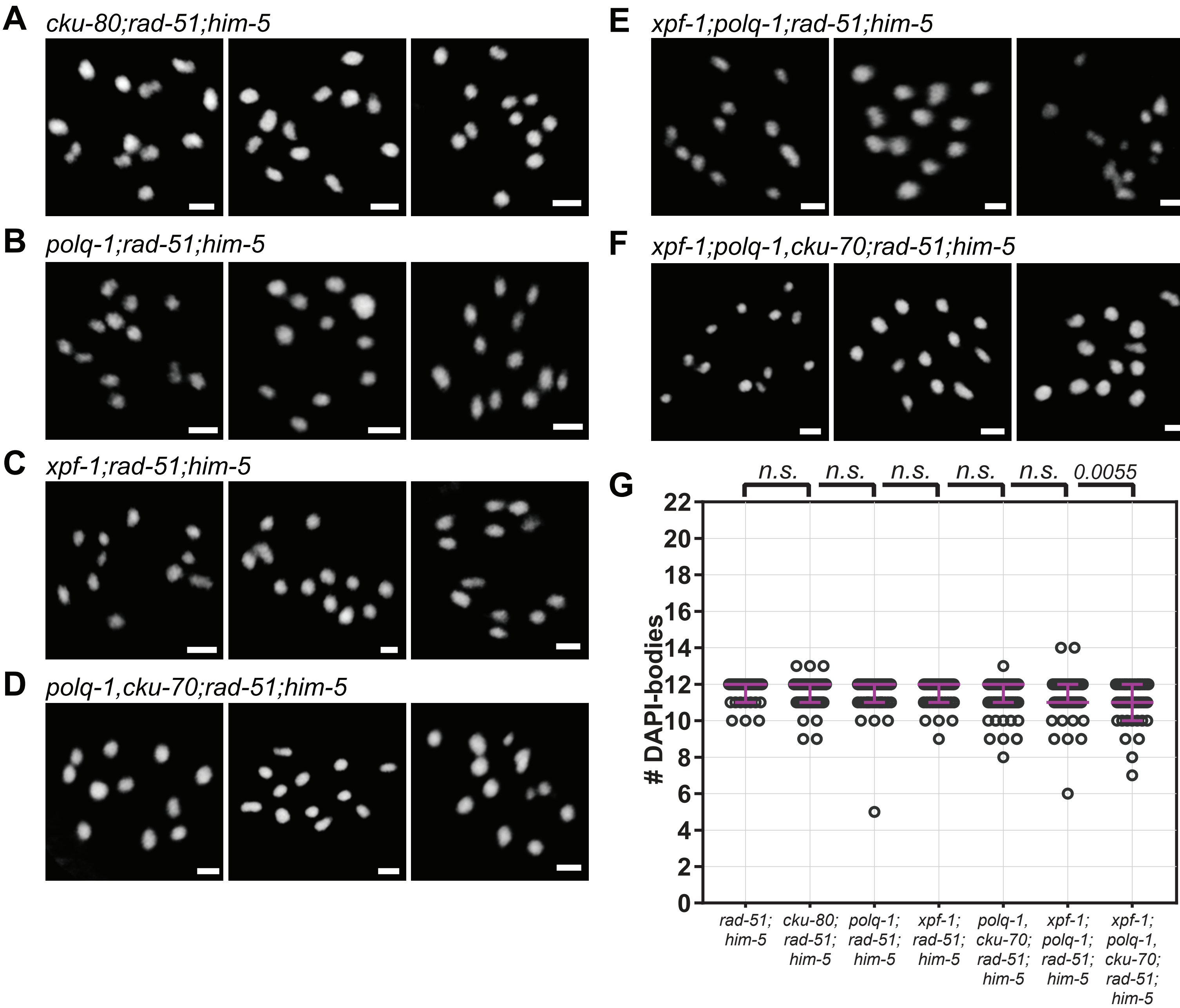

Figure S5 c-NHEJ, TMEJ, and SSA function redundantly to control repair in *rad-51;him-5* mutants under low DSB conditions (A-F) DAPI-stained diakinesis nuclei of two-day-old, irradiated adults of designated genotypes. Scale bars= 2μm. (G) Quantification of nuclei in (A-F). While depleting any single pathway does not have an impact on chromosome morphology in *rad-51;him-5*, impairment of all three pathways increases the occurrence of chromosome fusions. Magenta bars indicate median and interquartile range. Kruskal-Wallis multiple comparisons to *rad-51;him-5* (n.s.: not significant, P>0.06). *rad-51(lg8701);him-5(e1490)* (n=33), *cku-80(ok851);rad-51(lg8701);him-5(e1490)* (n=61), *polq-1(tm2027);rad-51(lg8701);him-5(e1490)* (n=60), *xpf-1(e1487);rad-51(lg8701);him-5(e1490)* (n=37), *polq-1(tm2026),cku-70(tm1524);rad-51(lg8701);him-5(e1490)* (n=61), *xpf-1(e1487); polq-1(tm2026);rad-51(lg8701);him-5(e1490)* (n=50), and *xpf-1(e1487); polq-1(tm2026),cku-70(tm1524);rad-51(lg8701);him-5(e1490)* (n=40).

FIGURE S6

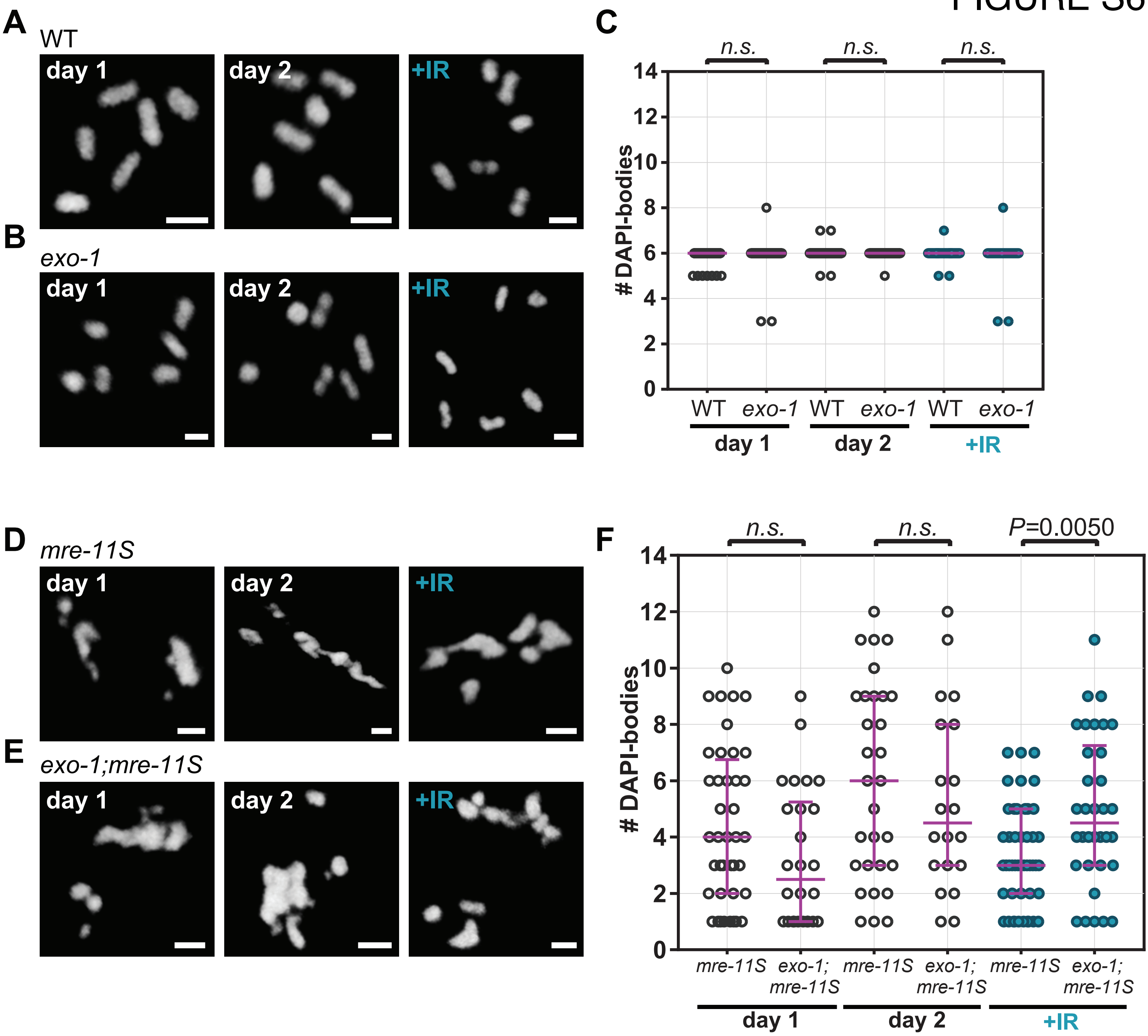

Figure S6 Role of EXO-1 in repair. (A-C) *exo-1* is dispensable for repair of DSBs in an otherwise wild-type background. (A, B) Representative images and (C) Quantification of diakinesis nuclei of one- and two-day-old, adults with and without IR. WT day 1 (n=74), *exo-1(tm1842)* day 1 (n=30), WT day 2 (n=45), *exo-1* day 2 (n=30), WT +IR (n=52), *exo-1* +IR (n=30). Two-tailed Mann-Whitney tests (n.s.: not significant, P>0.48). (D-F) EXO-1 is important to repair IR-induced MRE-11-processed breaks. Upon IR, chromosomes in *mre-11S* mutants have a lower tendency to form fusions if *exo-1* is depleted. (D, E) Representative images and (F) Quantification of DAPI bodies in diakinesis oocytes: *mre-11(iow1)* day 1 (n=40), *exo-1(tm1842);mre-11S* day 1 (n=26), *mre-11S* day 2 (n=30), *exo-1;mre-11S* day 2 (n=20), *mre-11S* +IR (n=47), *exo-1;mre-11S* +IR (n=34). P-values calculated from two-tailed Mann-Whitney tests (n.s.: not significant, P>0.08). Scale bars= 2μm. Dot-plot: Magenta bars indicate median and interquartile range.

Table S1: Strains used in this study

Genotype	Laboratory stock #
brc-2(tm1086) III/hT2 [bli-4(e937) let-?(q782) qIs48] (I;III)	QP0359
brc-2(tm1086 III/hT2 [bli-4(e937) let-?(q782) qIs48] (I;III); him-5(e1490) V	QP1862
cku-70(tm1524) III	QP1381
cku-70(tm1524) III;rad-51(lg8701) IV*/ nT1 [unc-?(n754) let-? qIs50] (IV;V).*	QP1671
cku-80(ok861) III	QP0842
cku-80(ok861) III;rad-51(lg8701)/ nT1 [unc-?(n754) let-? qIs50] (IV;V)	QP1107
cku-80(ok861);rad-51(lg8701) IV/nT1[unc-?(n754) let-? qIs50] (IV;V);him-5(e1490) V/nT1 unc-?(n754) let-? qIs50] (IV;V)	QP1073
dsb-2(me96) II	QP0938
dsb-2(me96) II;rad-51(lg8701),rec-8(ok978) IV/nT1[unc-?(n754) let-? qIs50] (IV;V)	QP1350
dsb-2(me96) II;rad-51(lg8701) IV/nT1[unc-?(n754) let-? qIs50] (IV;V)	QP1345
exo-1(tm1842) III	QP0901
exo-1(tm1842) III;mre-11(iow1),him-5(e1490) V/nT1[unc-?(n754) let-? qIs50] (IV;V)	QP1346
exo-1(tm1842) III;mre-11(iow1) V/nT1[unc-?(n754) let-? qIs50] (IV;V)	QP1698
exo-1(tm1842) III;rad-51(lg8701) IV/nT1[unc-?(n754) let-? qIs50] (IV;V)	QP1656
exo-1(tm1842) III;rad-51(lg8701) IV/ nT1[unc-?(n754) let-? qIs50] (IV;V);him-5(e1490) V/ nT1 [unc-?(n754) let-? qIs50] (IV;V)	QP1657
exo-1(tm1842) III;rad-51(lg8701) IV/nT1[unc-?(n754) let-? qIs50] (IV;V);mre-11(iow1),him-5(e1490) V/nT1[unc-?(n754) let-? qIs50] (IV;V)	QP1658
him-5(e1490) V	QP0421
him-5(ea42) V	QP1398
him-5(ok1896) V	QP0432
mre-11(iow1),him-5(e1490) V/nT1[unc-?(n754) let-? qIs50] (IV;V)	QP1116
mre-11(Iow1)/nT1[qIs51] (IV;V)	QP0900
polq-1(tm2026) III	QP1244
polq-1(tm2026),cku-70(tm1524) III;rad-51(lg8701) IV/nT1[unc-?(n754) let-? qIs50] (IV;V)	QP1592
polq-1(tm2026),cku-70(tm1524) III;rad-51(lg8701) IV/nT1 [unc-?(n754) let-? qIs50] (IV;V);him-5(e1490) V/ nT1[unc-?(n754) let-? qIs50] (IV;V)	QP1593
polq-1(tm2026) III;rad-51(lg8701) IV/nT1[unc-?(n754) let-? qIs50] (IV;V)	QP1341
polq-1(tm2026) III;rad-51(lg8701) IV/nT1[unc-?(n754) let-? qIs50] (IV;V);him-5(e1490) V/nT1[unc-?(n754) let-? qIs50] (IV;V)	QP1547

rad-51(lg8701),rec-8(ok978) IV/ nT1[unc-?(n754) let-? qIs50] (IV;V)	QP1347
rad-51(lg8701),rec-8(ok978) IV/nT1[unc-?(n754) let-? qIs50] (IV;V);him-5(e1490) V/nT1[unc-?(n754) let-? qIs50] (IV;V)	QP1351
rad-51(lg8701 IV)/nT1g;mre-11(iow1) V/nT1g	QP1697
rad-51(lg8701) IV/nT1[unc-?(n754) let-? qIs50]	QP1165
rad-51(lg8701) IV/nT1[unc-?(n754) let-? qIs50]; him-5(e1490) V/nT1[unc-?(n754) let-? qIs50] (IV;V)	QP1111
rad-51(lg8701) IV/nT1[unc-?(n754) let-? qIs50]; him-5(ea42) V/ nT1[unc-?(n754) let-? qIs50]	QP1411
rad-51(lg8701) IV/nT1[unc-?(n754) let-? qIs50]; him-5(ok1896) V/nT1[unc-?(n754) let-? qIs50]	QP1170
rad-51(lg8701)/nT1[unc-?(n754) let-? qIs50];mre-11(iow1),him-5(e1490)/nT1[unc-?(n754) let-? qIs50]	QP1112
rad-51(lg8701) IV/nT1[unc-?(n754) let-? qIs50];mre-11(iow1) IV/nT1[unc-?(n754) let-? qIs50]	QP1696
rec-8(ok978) IV/nT1[unc-?(n754) let-? qIs50]	QP1297
spo-11(me44),rec-8(ok978) IV/nT1 [qIs51] (IV;V)	QP1348
spo-11(me44) IV/nT1 [qIs51] (IV;V)	QP0963
xpf-1(e1487) II	QP0965
xpf-1(e1487) II;cku-80(ok861) III;rad-51(lg8701 IV)/nT1[unc-?(n754) let-? qIs50];him-5(e1490) V/nT1[unc-?(n754) let-? qIs50]	QP1377
xpf-1(e1487) II;polq-1(tm2026),cku-70(tm1524)III; him-5(e1490) V/nT1[unc-?(n754) let-? qIs50]	QP1595
xpf-1(e1487) II;polq-1(tm2026),cku-70(tm1524) III; rad-51(lg8701) IV/nT1[unc-?(n754) let-? qIs50]	QP1594/QP1700/ QP1701
xpf-1(e1487) II;polq-1(tm2026),cku-70(tm1524) III; rad-51(lg8701 IV)/nT1[unc-?(n754) let-? qIs50]; him-5(e1490) V/nT1[unc-?(n754) let-? qIs50]	QP1596/QP1612
xpf-1(e1487) II;polq-1(tm2026) III;rad-51(lg8701) IV/nT1[unc-?(n754) let-? qIs50];him-5(e1490)/nT1[unc-?(n754) let-? qIs50]	QP1376
xpf-1(e1487) II;rad-51(lg8701) IV/nT1[unc-?(n754) let-? qIs50]	QP1167
xpf-1(e1487) II;rad-51(lg8701) IV/nT1[unc-?(n754) let-? qIs50]; him-5(e1490) V/nT1[unc-?(n754) let-? qIs50]	QP1113
rfs-1(ok1372),helq-1(tm2134) III	QP1100
rfs-1(ok1372),helq-1(tm2134) III;him-5(ok1896) V	QP1060
rad-54(ok615) I	QP649
rad-54(ok615) I;him-5(ok1896) V	QP1004

Table S2

PCR program: 94^4min-(94^t-Tm^t-72^2t)x#cycles-72^4t-4^10-end

gene	allele	primers name and sequence	Tm (◦C)	t (sec)	#cycles	Band size in wild type (bp)	Band size in mutant (bp)	Gel concentration (% is grams of agarose powder per 100 mL TAE Buffer)	Notes
cku-70	tm1524	ZK-167 5'-GAGCTATTCAGGTTCAAATTTGATGC-3' ZK-194 5'-GCGGTACTGCCAAGTGTTGTCTG-3'	58	30	40	431	0	1%	Wild type specific PCR.
cku-70	tm1524	NM-099 5'-CTCGATTCGCAACCGTCG-3' NM-100 5'-GATGAGTCTGCTTGAGCAC-3'	63	30	45	1471	694	1%	May not amplify WT band in a heterozygote individual.
cku-80	ok861	ZK-170 5'-GGTGTTCTGGGAGCCGTCG-3' ZK-171 5'-AGCGCGTGTCCTTCTATCCCTAT-3'	58	30	40	0	441	1%	Mutant specific PCR. Also works at Tm55 although a faint band may appear around 300 bp when mutation is absent.
cku-80	ok861	ZK-170 5'-GGTGTTCTGGGAGCCGTCG-3' ZK-172 5'-CGGTAGCCGGTCTTGACACG	58	30	40	556	N/A	1%	Wild type specific PCR.
dsb-2	me96	TSM-203 5'-CCTAGACGCGTACTAGTCGACTCCTGAAAGTTGAGATGTACTACAAACT-3' TSM-204 5'-TTGGAATCATAGTGTAAATCCACC-3' TSM-205 5'-CTGCCTGAAAGTTGAGATGTACTACGAATA-3'	55	15	40	201	194	3%	Run the agarose gel at low voltage and for a long time to separate the bands properly.
exo-1	tm1842	ZK-216 5'-GGTCGCAATCGATGTGAGTTGC-3' ZK-217 5'-GCAGCTGTGCTCAACCCGAC-3'	58	15	35	782	220	1%	May not amplify WT band in a heterozygote individual.
exo-1	tm1842	ZK-216 5'-GGTCGCAATCGATGTGAGTTGC-3' ZK-218 5'-GCAGCTCACGACGCTCCTC-3'	58	15	35	265	0	1%	Wild type specific PCR.
him-5	e1490	ZK-108 5'-CAGTGCATGGAATTTTACTGATTATTTTCCGA-3' ZK-109 5'-TGCGTCTATCAGCTTCGTCATTG-3' ZK-138 5'-TAGACGCGTACTAGTCGACTAACATGGAATTTTACTGATTATTTTCTAG-3'	55	15	40	~150	<150	3%	3 primers PCR to genotype a point mutation.
him-5	ea42	NM-087 5'-CGTTGCGATACCATCTTCTC-3' ZK-20 5'-CGATGCGACCAACTGTTTTTCG-3'	58	15	40	375	0	1%	Wild type specific PCR.
him-5	ea42	NM-087 5'-CGTTGCGATACCATCTTCTC-3' NM-088 5'-CCACGAATTATTGAGCGCG-3'	58	15	40	1568	157	1%	Mutant band migrates very quickly on gel. May not amplify WT band in a heterozygote individual.
him-5	ok1896	ZK-16 5'-CGGAGCTCAAAATGAAAAGAGCAGC-3' ZK-20 5'-CGATGCGACCAACTGTTTTTCG-3'	58	30	35	842	324	1%	May not amplify WT band in a heterozygote individual.
him-5	ok1896	ZK-16 5'-CGGAGCTCAAAATGAAAAGAGCAGC-3' JXG-76 5'-GGAAATGGTTCATTAATTACCGCG-3'	58	30	35	299	0	1%	Wild type specific PCR.
mre-11	iow1	ZK-242 5'-CAATTTGAAGCACTTCTTCAAAAGTG-3' ZK-251 5'-CTATCATCAAAATTCTCGTTGCCGT-3' ZK-252 5'-CCTAGACGCGTACTAGTCGACTGACATCATCAAAATTCTCGTTGCTAC-3'	58	15	40	~200	<200	3%	3 primers PCR to genotype a point mutation.
polq-1	tm2026	NM-068 5'-TTCTGAAAACATCACCGTACAT-3' NM-069 5'-GTTCATGTAGGATTCGGG-3'	60	15	50	1331	417	1%	Needs more DNA to work properly. Single worm genotyping is tricky.
polq-1	tm2026	NM-068 5'-TTCTGAAAACATCACCGTACAT-3' NM-070 5'-TGTTTGAAGACATCCACGAG-3'	58	30	40	581	0	1%	Wild type specific PCR.
rad-51	lg8701	ZK-74 5'-CATCTTACCTCATTCTTGGCCGCTT-3' ZK-75 5'-GCCACAGTCTGGCAGTCTTGTGTC-3'	65	30	35	1725	724	1%	May not amplify WT band in a heterozygote individual.
rec-8	ok978	NM-082 5'-GGTAATTGCCGACTTCAGC-3' NM-083 5'-AGTCCGTTCTTCATCCTCG-3'	58	30	40	1120	714	1%	May not amplify WT band in a heterozygote individual.
rec-8	ok978	NM-082 5'-GGTAATTGCCGACTTCAGC-3' NM-084 5'-CGGTCGCACAGTTGAATGA-3'	58	30	40	601	0	1%	Wild type specific PCR.
rec-8	ok978	NM-082 5'-GGTAATTGCCGACTTCAGC-3' NM-085 5'-TGAGCGTTGACTGAAACCTAAT-3'	58	30	40	0	481	1%	Mutant specific PCR
spo-11	me44	WL-15 5'-CGATCGAGGAATCATCTTCTC-3' WL-16 5'-GCCAACGATTGAATGGAGCGA-3' WL-17 5'-GTTGCAAGTTGTTACTAGTTCCAACGATTGAATGGATCTG-3'	59	15	40	189	178	3%	3 primers PCR to genotype a point mutation.
xpf-1	e1487	ZK-96 5'-GGACAGTACTCTCGGAGATT-3' ZK-98 5'-CACATTGTCCGCTTGTGTC-3'	58	30	40	0	~800	1%	Mutant specific PCR.
xpf-1	e1487	ZK-96 5'-GGACAGTACTCTCGGAGATT-3' ZK-97 5'-CGAACTGTATCAAATTGGTCTG-3'	58	30	40	~950	0	1%	Wild type specific PCR.

Table S3

Figure #	Comparision	Test	q value	individual P value	Result	Global P value
S1	rad-51(lg8701);him-5(e1490) vs. rad-51(lg8701);him-5(ok1896)	Kruskall-Wallis multicomparision test, corrected by two-stage step-up method of Benjamini, Krieger and Yekutieli	0.2113	0.3018	n.s.	0.0215
	rad-51(lg8701);him-5(e1490) vs. rad-51(lg8701);him-5(ea42)		0.0135	0.0065	significant	
	rad-51(lg8701);him-5(ok1896) vs. rad-51(lg8701);him-5(ea42)		0.1195	0.1138	n.s.	
S1	dsb-2(me96) vs. WT	Two-tailed Mann-Whitney		<0.0001	significant	
S1	dsb-2(me96) +IR vs. WT +IR	Two-tailed Mann-Whitney		0.5567	n.s.	
2	rad-51(lg8701);him-5(e1490) +IR vs. rad-51(lg8701) +IR	Two-tailed Mann-Whitney		<0.0001	significant	
2	rad-51(lg8701);him-5(e1490) +IR vs rad-51(lg8701);him-5(e1490)	Two-tailed Mann-Whitney		<0.0001	significant	
S2	rad-51(lg8701);him-5(e1490) +IR vs. rad-51(lg8701);him-5(ok1896) +IR	Kruskall-Wallis multicomparision test, corrected by two-stage step-up method of Benjamini, Krieger and Yekutieli	0.8188	0.4178	n.s.	0.7023
	rad-51(lg8701);him-5(e1490) +IR vs. rad-51(lg8701);him-5(ea42) +IR		0.9811	0.9344	n.s.	
	rad-51(lg8701);him-5(ok1896) +IR vs. rad-51(lg8701);him-5(ea42) +IR		0.8188	0.5199	n.s.	
S2	mre-11S(iow1) vs mre-11S(iow1),him-5(e1490)	Two-tailed Mann-Whitney		<0.0001	significant	
	mre-11S(iow1) +IR vs mre-11S(iow1),him-5(e1490) +IR	Two-tailed Mann-Whitney		<0.0001	significant	
S4	cku-70(tm1524) vs. WT	Two-tailed Mann-Whitney		0.6851	n.s.	
	cku-80(ok861) vs. WT	Two-tailed Mann-Whitney		0.3435	n.s.	
4	cku-70(tm1524);rad-51(lg8701) vs. rad-51(lg8701)	Kruskall-Wallis multicomparision test, corrected by two-stage step-up method of Benjamini, Krieger and Yekutieli	0.0005	0.0005	significant	0.0005
	cku-80(ok861);rad-51(lg8701) vs. rad-51(lg8701)		0.0026	0.0050	significant	
	cku-70(tm1524);rad-51(lg8701) vs. cku-80(ok861);rad-51(lg8701)		0.1740	0.4971	n.s.	
S4	polq-1(tm2026) vs WT	Two-tailed Mann-Whitney		0.6882	n.s.	
	xpf-1(e1487) vs WT	Two-tailed Mann-Whitney		0.0002	significant	
4	rad-51(lg8701) vs. cku-70(tm1524);rad-51(lg8701)	Kruskall-Wallis multicomparision test, corrected by two-stage step-up method of Benjamini, Krieger and Yekutieli	0.0012	0.0013	significant	<0,0001
	rad-51(lg8701) vs. polq-1(tm2026);rad-51(lg8701)		0.0012	0.0013	significant	
	rad-51(lg8701) vs. xpf-1(e1487);rad-51(lg8701)		<0.0001	<0.0001	significant	
	rad-51(lg8701) vs. polq-1(tm2026),cku-70(tm1524);rad-51(lg8701)		0.003	0.0046	significant	
	rad-51(lg8701) vs. xpf-1(e1487);polq-1(tm2026),cku-70(tm1524);rad-51(lg8701)		<0.0001	<0.0001	significant	
	cku-70(tm1524);rad-51(lg8701) vs. polq-1(tm2026);rad-51(lg8701)		0.2949	0.8425	n.s.	
	cku-70(tm1524);rad-51(lg8701) vs. xpf-1(e1487);rad-51(lg8701)		0.0007	0.0005	significant	
	cku-70(tm1524);rad-51(lg8701) vs. polq-1(tm2026),cku-70(tm1524);rad-51(lg8701)		0.2488	0.6634	n.s.	
	cku-70(tm1524);rad-51(lg8701) vs. xpf-1(e1487);polq-1(tm2026),cku-70(tm1524);rad-51(lg8701)		0.0482	0.101	n.s.	
	polq-1(tm2026);rad-51(lg8701) vs. xpf-1(e1487);rad-51(lg8701)		0.0013	0.0018	significant	
	polq-1(tm2026);rad-51(lg8701) vs. polq-1(tm2026),cku-70(tm1524);rad-51(lg8701)		0.2176	0.5387	n.s.	
	polq-1(tm2026);rad-51(lg8701) vs. xpf-1(e1487);polq-1(tm2026),cku-70(tm1524);rad-51(lg8701)		0.0848	0.1938	n.s.	
	xpf-1(e1487);rad-51(lg8701) vs. polq-1(tm2026),cku-70(tm1524);rad-51(lg8701)		0.0001	<0.0001	significant	
	xpf-1(e1487);rad-51(lg8701) vs. xpf-1(e1487);polq-1(tm2026),cku-70(tm1524);rad-51(lg8701)		0.0084	0.0144	significant	
	polq-1(tm2026),cku-70(tm1524);rad-51(lg8701) vs. xpf-1(e1487);polq-1(tm2026),cku-70(tm1524);rad-51(lg8701)		0.0139	0.0266	significant	
In text	rad-51(lg8701) vs. rad-51(lg8701) +IR	Two-tailed Mann-Whitney		0.4933	n.s.	
S5	rad-51(lg8701);him-5(e1490) vs. cku-80(ok861);rad-51(lg8701);him-5(e1490)	Kruskall-Wallis multicomparision test, corrected by two-stage step-up method of Benjamini, Krieger and Yekutieli	0.8191	0.7917	n.s.	0,0103
	rad-51(lg8701);him-5(e1490) vs. polq-1(tm2027);rad-51(lg8701);him-5(e1490)		0.8191	0.9361	n.s.	
	rad-51(lg8701);him-5(e1490) vs. xpf-1(e1487);rad-51(lg8701);him-5(e1490)		0.5676	0.4324	n.s.	
	rad-51(lg8701);him-5(e1490) vs. polq-1(tm2027),cku-70(tm1524);rad-51(lg8701);him-5(e1490)		0.2334	0.1333	n.s.	
	rad-51(lg8701);him-5(e1490) vs. xpf-1(e1487);polq-1(tm2027);rad-51(lg8701);him-5(e1490)		0.1651	0.0629	n.s.	
	rad-51(lg8701);him-5(e1490) vs. xpf-1(e1487);polq-1(tm2027),cku-70(tm1524);rad-51(lg8701);him-5(e1490)		0.029	0.0055	significant	
5	rad-51(lg8701);him-5(e1490) +IR vs. cku-80(ok861);rad-51(lg8701);him-5(e1490) +IR	Kruskall-Wallis multicomparision test, corrected by two-stage step-up method of Benjamini, Krieger and Yekutieli	0.0358	0.0256	significant	<0,0001
	rad-51(lg8701);him-5(e1490) +IR vs. polq-1(tm2027);rad-51(lg8701);him-5(e1490) +IR		0.0567	0.054	n.s.	
	rad-51(lg8701);him-5(e1490) +IR vs. xpf-1(e1487);rad-51(lg8701);him-5(e1490) +IR		0.0796	0.0948	n.s.	
	rad-51(lg8701);him-5(e1490) +IR vs. polq-1(tm2027),cku-70(tm1524);rad-51(lg8701);him-5(e1490) +IR		0.0028	0.0007	significant	
	rad-51(lg8701);him-5(e1490) +IR vs. xpf-1(e1487);polq-1(tm2027);rad-51(lg8701);him-5(e1490) +IR		0.4618	0.6597	n.s.	
	rad-51(lg8701);him-5(e1490) +IR vs. xpf-1(e1487);polq-1(tm2027),cku-70(tm1524);rad-51(lg8701);him-5(e1490) +IR		0.0297	0.0141	significant	
S6	exo-1(tm1842) vs. WT [day 1 adults]	Two-tailed Mann-Whitney		0.4813	n.s.	
S6	exo-1(tm1842) vs. WT [day 2 adults]	Two-tailed Mann-Whitney		0.6718	n.s.	
S6	exo-1(tm1842) +IR vs. WT +IR	Two-tailed Mann-Whitney		0.7164	n.s.	
S6	mre-11S(iow1) vs. exo-1(tm1842);mre-11S(iow1) [day 1 adults]	Two-tailed Mann-Whitney		0.0818	n.s.	
S6	mre-11S(iow1) vs. exo-1(tm1842);mre-11S(iow1) [day 2 adults]	Two-tailed Mann-Whitney		0.5242	n.s.	
S6	mre-11S(iow1) +IR vs. exo-1(tm1842);mre-11S(iow1) +IR	Two-tailed Mann-Whitney		0.0050	significant	
6	rad-51(lg8701);mre-11S(iow1) vs. rad-51(lg8701)	Kruskall-Wallis multicomparision test, corrected by two-stage step-up method of	0.0008	0.0004	singificant	0.0007
	exo-1(tm1842);rad-51(lg8701) vs. rad-51(lg8701)		0.0119	0.0113	singificant	
6	rad-51(lg8701);him-5(e1490) vs. rad-51(lg8701);mre-11S(iow1),him-5(e1490)	Kruskall-Wallis multicomparision test, corrected by two-stage step-up method of Benjamini, Krieger and Yekutieli	0.2875	0.1825	n.s.	0.1279
	rad-51(lg8701);him-5(e1490) vs. exo-1(tm1842);rad-51(lg8701);him-5(e1490)		0.1186	0.0188	n.s.	
	rad-51(lg8701);him-5(e1490) vs. exo-1(tm1842);rad-51(lg8701);mre-11S(iow1),him-5(e1490)		0.4232	0.3359	n.s.	
	rad-51(lg8701);mre-11S(iow1),him-5(e1490) vs. exo-1(tm1842);rad-51(lg8701);him-5(e1490)		0.2875	0.1764	n.s.	
	rad-51(lg8701);mre-11S(iow1),him-5(e1490) vs. exo-1(tm1842);rad-51(lg8701);mre-11S(iow1),him-5(e1490)		0.7307	0.6959	n.s.	
	exo-1(tm1842);rad-51(lg8701);him-5(e1490) vs. exo-1(tm1842);rad-51(lg8701);mre-11S(iow1),him-5(e1490)		0.2875	0.1005	n.s.	
6	rad-51(lg8701);him-5(e1490) +IR vs. rad-51(lg8701);mre-11S(iow1),him-5(e1490) +IR	Kruskall-Wallis multicomparision test, corrected by two-stage step-up method of Benjamini, Krieger and Yekutieli	0.008	0.0114	significant	<0,0001
	rad-51(lg8701);him-5(e1490) +IR vs. exo-1(tm1842);rad-51(lg8701);him-5(e1490) +IR		0.2744	0.7841	n.s.	
	rad-51(lg8701);him-5(e1490) +IR vs. exo-1(tm1842);rad-51(lg8701);mre-11S(iow1),him-5(e1490) +IR		0.0051	0.0049	significant	
	rad-51(lg8701);mre-11S(iow1),him-5(e1490) +IR vs. exo-1(tm1842);rad-51(lg8701);him-5(e1490) +IR		0.0081	0.0155	significant	
	rad-51(lg8701);mre-11S(iow1),him-5(e1490) +IR vs. exo-1(tm1842);rad-51(lg8701);mre-11S(iow1),him-5(e1490) +IR		<0.0001	<0.0001	significant	
	exo-1(tm1842);rad-51(lg8701);him-5(e1490) +IR vs. exo-1(tm1842);rad-51(lg8701);mre-11S(iow1),him-5(e1490) +IR		0.0182	0.0432	significant	
7	dsb-2(me96);rad-51(lg8701) vs dsb-2(me96);rad-51(lg8701) +IR	Two-tailed Mann-Whitney		0.1674	n.s.	